Environmental Pollution 233 (2018) 1058–1067

Contents lists available at ScienceDirect

Environmental Pollution

journal homepage: www.elsevier.com/locate/envpol

Source apportionment for fine particulate matter in a Chinese city using an improved gas-constrained method and comparison with multiple receptor models☆

Guoliang Shi [a], Jiayuan Liu [a], Haiting Wang [a], Yingze Tian [a], Jie Wen [a], Xurong Shi [a], Yinchang Feng [a, *], Cesunica E. Ivey [b], Armistead G. Russell [c]

[a] State Environmental Protection Key Laboratory of Urban Ambient Air Particulate Matter Pollution Prevention and Control & Center for Urban Transport Emission Research, College of Environmental Science and Engineering, Nankai University, Tianjin, China
[b] Department of Physics, University of Nevada Reno, Reno, NV 89557, USA
[c] School of Civil and Environmental Engineering, Georgia Institute of Technology, Atlanta, GA 30332-0512, USA

ARTICLE INFO

Article history:
Received 20 June 2017
Received in revised form
3 October 2017
Accepted 3 October 2017
Available online 13 October 2017

Keywords:
CMBGC-Iteration
CMB-GC
Receptor model
Source apportionment

ABSTRACT

$PM_{2.5}$ is one of the most studied atmospheric pollutants due to its adverse impacts on human health and welfare and the environment. An improved model (the chemical mass balance gas constraint-Iteration: CMBGC-Iteration) is proposed and applied to identify source categories and estimate source contributions of $PM_{2.5}$. The CMBGC-Iteration model uses the ratio of gases to PM as constraints and considers the uncertainties of source profiles and receptor datasets, which is crucial information for source apportionment. To apply this model, samples of $PM_{2.5}$ were collected at Tianjin, a megacity in northern China. The ambient $PM_{2.5}$ dataset, source information, and gas-to-particle ratios (such as $SO_2/PM_{2.5}$, $CO/PM_{2.5}$, and $NOx/PM_{2.5}$ ratios) were introduced into the CMBGC-Iteration to identify the potential sources and their contributions. Six source categories were identified by this model and the order based on their contributions to $PM_{2.5}$ was as follows: secondary sources (30%), crustal dust (25%), vehicle exhaust (16%), coal combustion (13%), SOC (7.6%), and cement dust (0.40%). In addition, the same dataset was also calculated by other receptor models (CMB, CMB-Iteration, CMB-GC, PMF, WALSPMF, and NCAPCA), and the results obtained were compared. Ensemble-average source impacts were calculated based on the seven source apportionment results: contributions of secondary sources (28%), crustal dust (20%), coal combustion (18%), vehicle exhaust (17%), SOC (11%), and cement dust (1.3%). The similar results of CMBGC-Iteration and ensemble method indicated that CMBGC-Iteration can produce relatively appropriate results.

1. Introduction

In the past decade, airborne particulate matter (PM) has become one of the most important pollutants in the world due to its serious effects on visibility (Kanakidou et al., 2005), global climate change (Seinfeld and Pandis, 1998), and human health (Monn, 2001; Nel, 2005; Lim et al., 2012). For example, some reports have demonstrated that PM could lead to asthma and cardiovascular diseases by entering into the human respiratory tract and lungs (Arruti et al., 2011; Nelin et al., 2012; Van Ryswyk et al., 2014; Wang et al., 2017). It can also cause visibility degradation through the scattering and absorption of solar radiation (Hinwood et al., 2014; Revuelta et al., 2014; de Paula et al., 2015; Liberda et al., 2015). PM, especially $PM_{2.5}$, (particles with an aerodynamic diameter of <2.5 μm) pollution is becoming more severe with rapid economic and industrial development (Chen et al., 2015; Singh et al., 2017). $PM_{2.5}$ emitted directly from natural and anthropogenic activities usually varies in toxicity because $PM_{2.5}$ is a complex mixture of pollutants with different physical, chemical, and biological compositions (Zhou et al., 2011; Krall et al., 2013). It is necessary to understand the potential emission sources that contribute to the increasing daily $PM_{2.5}$ levels (Zheng et al., 2005). The results of source apportionment can provide policy makers with scientific information, help establish regional emission control strategies,

☆ This paper has been recommended for acceptance by Eddy Y. Zeng.
* Corresponding author.
E-mail address: fengyc@nankai.edu.cn (Y. Feng).

https://doi.org/10.1016/j.envpol.2017.10.007
0269-7491/

and design efficient management measures.

Receptor models are the most commonly used source apportionment (SA) techniques (Kong et al., 2010a; Pant and Harrison, 2012; Belis et al., 2013; Heo et al., 2017), which identify and apportion atmospheric pollutant emissions by solving a mass conservation equation (Schauer et al., 1996; Kong et al., 2010b; Pant and Harrison, 2012). Historically, receptor models mainly include the chemical mass balance (CMB) model (Watson, 1984, Watson et al., 2002) and factor analytic (FA) approaches such as positive matrix factorization (PMF) and UNMIX (Hopke, 2003; Kong et al., 2012; Hasheminassab et al., 2014; Bari and Kindzierski, 2016; Shi et al., 2016a). The CMB model uses an effective variance least squares approach and is only applicable when the number and nature of the sources are known (Watson et al., 2002). CMB has been widely used in SA applications in several regions of the world (Chen et al., 2007; Zheng et al., 2007; Harrison et al., 2011; Gugamsetty et al., 2012; Shi et al., 2012). Studies have compared receptor model results. Shi et al. (2014) developed multiple combined models, including the PCA/MLR-CMB, Unmix-CMB and PMF-CMB models, which indicated the combination of various methods could provide more information for source apportionment than individual methods (Shi et al., 2014). Cesari et al. (2016a) compared PMF and PCA models. The results showed that PMF results typically have good stability, while PCA results are more sensitive to chemical components. In addition, Cesari et al. (2016b) showed that SA, based on several receptor models, could get more stable results than a single model. These receptor models consider the physical and chemical characteristics of PM to identify source categories and apportion their contribution; however, gaseous pollutants are not involved.

An improved CMB approach, called CMB-GC, uses CMB and introduces ambient gas-phase pollutants (SO_2, CO, NOx) to constrain results (Marmur et al., 2005). CMB-GC takes into account gaseous pollutants, increasing the discrimination of the sources. Source indicative ratios including $SO_2/PM_{2.5}$, $CO/PM_{2.5}$, and $NOx/PM_{2.5}$ are used as constraints, which assist in identifying emission sources that may have similar $PM_{2.5}$ emissions but may have significantly different gaseous emissions. More accurate results are obtained by incorporating gaseous pollutant constraints. However, CMB-GC does not incorporate the uncertainty of the source profiles and the receptor data. Uncertainty estimates are key parameters in SA, and practice has shown that uncertainty substantially impacts SA results (Belis et al., 2015a, 2015b; Shi et al., 2016b). In the field of environmental science, uncertainty can represent the physical reality, and various types of information can be communicated to the model (Paatero and Tapper, 1994; Cheng and Sandu, 2009). The uncertainty of receptor data is influenced by many factors including ambient sampling, instrumentation, sample analysis, and data processing. In addition, source profile uncertainty is also caused by source category errors. Uncertainty is a very important parameter for ambient samples, and model results are more stable after incorporating uncertainties. (Lee and Russell, 2007).

In this study, an improved model CMBGC-Iteration was derived from the CMB-GC model. The uncertainties of the ambient dataset and source profiles were incorporated into the iterative solution. The convergence results were obtained and made the results of the source apportionment more stable. The improved model was then applied to a specific receptor data set. We evaluated the emission source contributions to $PM_{2.5}$ using the CMBGC-Iteration model and compared source apportionment results with multiple receptor models including CMBGC, CMB-Iteration, CMB models, PMF, NCAPCA, and WALSPMF.

To summarize, the main research contents of this paper are: (1) proposing an improved CMBGC-Iteration model; (2) using the improved model to identify and characterize emission source categories and evaluate contributions of each source to $PM_{2.5}$; (3) comparing the source apportionment results from CMBGC-Iteration with multiple models results for the same set of ambient data. Overall, results from various models and approaches along with model uncertainties can be used together to calculate ensemble-average source impacts.

2. Material and methods

2.1. The data for source apportionment

The sampling site (39°11′N, 117°17′E) is in a large industrial city Tianjin which is in the eastern part of the North China Plain, covering an area of about 11,300 square kilometers. By the end of 2015, the city's residential population was 15.47 million (data from the Tianjin Statistical Information Net). The monitoring site is one of the busiest traffic roads in Tianjin city. The study area is composed of a dense, mixed residential and commercial area, many premier educational institutes, and hospitals. Overall, this area has extensive human activities and heavy traffic.

Ambient $PM_{2.5}$ samples were collected on the roof of a laboratory building about 15 m high, and the sampling activities took place during the period from April 2014 to January 2015. A four-channel low volume air sampler (with flow of 16.7L/min) was used while the $PM_{2.5}$ samples were simultaneously collected by two of the four channels: one with quartz filters (diameter 47 mm) and the other with polypropylene membrane filters (diameter 47 mm). The sampler maintained a continuously running 24 h cycle, and filters were changed every 12 h at 8:00 (local time) in the morning and evening every day. A total of 228 valid $PM_{2.5}$ samples (the sum of quartz fiber filter samples and polypropylene membrane filter samples) were obtained during the sampling campaign. The quartz fiber filters were used for analyzing OC, EC, and water-soluble ions, and the polypropylene membrane filters were used for measuring elemental composition. Sample storage and chemical analysis methods are described in detail in our previous studies (Tian et al., 2013, 2016a) and supplementary material. One-hundred and fourteen receptor data points were obtained.

2.2. Principle of CMBGC-Iteration

The traditional CMB model is based on the chemical mass balance method. The source contributions are analyzed by determining the relationship between chemical species in $PM_{2.5}$, sources, and observations. The chemical mass balance (CMB) receptor model developed by the USA-EPA (EPA, 1987) has been widely used to identify potential source categories and source contributions of PM_{10} and $PM_{2.5}$ (Watson, 1984; Samara et al., 2003; Chen et al., 2007). The CMB model requires both ambient measurements and knowledge of the emission sources (source profiles). Under the assumption that reactions do not occur among the chemical species, the CMB model establishes a balance between emission sources and the ambient receptor data and then estimates the source contributions to PM (The USEPA, 2006; Louie et al., 2005; Watson et al., 2008). The CMB model can be expressed as follows:

$$C_i = \sum_{j=1}^{J} F_{ij} \cdot S_j \quad (1)$$

where J is the total number of emission sources; C_i is the ith species concentration measured at the ambient receptor; F_{ij} is the relative concentration of ith species in the jth source; and S_j is the contribution of jth source. The details of the CMB model are provided

elsewhere (The USEPA, 2006; Yatkin and Bayram, 2008).

CMB-GC (also called CMB-LGO, CMB-Lipschitz Global Optimizer) is an extension of the CMB model. According to Marmur's work (Marmur et al., 2005), gas-to-particle ratios can be used for source identification, such as the $SO_2/PM_{2.5}$, $CO/PM_{2.5}$, and $NO_x/PM_{2.5}$ ratios. Therefore, the principle of the CMB-GC model is dependent on the chemical mass balance method (Chow et al., 2007; Watson et al., 2001, 2008). This updated model can better quantify source contributions by incorporating gas constraints (Marmur et al., 2005).

The CMBGC-Iteration model is an improved version of the CMB-GC model. Compared with CMB-GC, the uncertainties of sources and observations are included in the solution of CMB-LGO, and the iteration produces more stable results. The detailed process of the CMBGC-Iteration method is described as follows, where superscript k is used to show the value of a variable at the *kth* iteration (in each iterative step, six stages are involved):

Stage (1). At the beginning of the calculation, set the initial estimate of source contributions to zero.

$$s_j^0 = 0 \tag{2}$$

Stage (2). Calculate the "effective variance" v_i^k based on the uncertainties from sources and observations.

$$v_i^k = \sigma_{c_i}^2 + \sum_{j=1}^{J} \left(s_j^k\right)^2 \cdot \sigma_{f_{ij}}^2 \quad i = 1, \ldots n, \;\; j = 1, \ldots m \tag{3}$$

The variables used are defined as: σ_{ci} is the standard deviation of the c_i measurement; $\sigma_{f_{ij}}^2$ is the standard deviation of the f_{ij} measurement; c_i is the concentration ($\mu g/m^3$) of the ith chemical species in the daily measurement; f_{ij} is the chemical profile of jth source category, indicating the fraction (g/g) of ith chemical compound in the jth source category; and J is the number of the source categories. Variables $c_i, f_{ij}, \sigma_{c_i}$, and $\sigma_{f_{ij}}$ are the input data of the model while s_j is the estimation.

Here, $\sigma_{c_i}^2$ represents the uncertainty in the observation while $\sum (s_j^k)^2 \cdot \sigma_{f_{ij}}^2$ describes the uncertainty of all the sources. Therefore, v_i^k can provide uncertainties of both the sources and observations. It should be noted that in Eq. (3), the source contribution s_j^k is involved in the calculation, and its values are indicators of the convergence of the iteration.

Stage (3). Calculate the weighted source profile using the "effective variance matrix" and observed concentrations.

In SA studies, the chemical species concentrations ($\mu g\ m^{-3}$) in the raw data should be weighted (usually by the standard deviation) to ensure the stability of the dataset. For example, consider two species such as Al and Si, both with a concentration of 10 $\mu g/m^3$; however the standard deviation for Al is 5 while Si is 2 $\mu g/m^3$. These two species should be weighted by their standard deviation. This way Al can be somehow down-weighted (due to its high uncertainties) compared with Si.

Here, raw source profiles and observations are weighted by v_i^k:

$$\left(c_i^*\right)^k = c_i \Big/ \sqrt{v_i^k}; \quad \left(f_{ij}^*\right)^k = f_{ij} \Big/ \sqrt{v_i^k} \tag{4}$$

where $(c_i^*)^k$ is the weighted concentration of the observations, and $(f_{ij}^*)^k$ is the weighted source fingerprint. After stage (3), all of the chemical species in $PM_{2.5}$ would be up- or down-weighted by the uncertainties. It should be noted that the weighted source profiles (and weighted observations) would change greatly during some iterative steps at the beginning, while being constant (only slightly varying) at the last two steps of iteration, which can also show the convergence.

Stage (4). Calculate source contributions based on the chemical mass balance and the gas-to-particle ratio constraint.

First, a balance between the sources and observations (receptor) is established:

$$\left(c_i^*\right)^k = \sum_{j=1}^{J} \left(s_j\right)^{k+1} \cdot \left(f_{ij}^*\right)^k \tag{5}$$

where $(s_j)^{k+1}$ is the estimated contribution of the jth source at the kth step.

In Eq. (5), gas-to-particle ratio constraints help identify source contributions. For each source category, the emitted gas concentrations can be calculated as (using SO_2 as an example):

$$[SO_2]_j = \left(s_j\right)^{k+1} \cdot R_j^{SO_2}; \quad R_j^{SO_2} = \left(\frac{SO_2}{PM_{2.5}}\right)_j \tag{6}$$

where $[SO_2]$ is the estimated concentration of SO_2 from the jth source category, and $R_j^{SO_2}$ is the gas-to-particle ratio—the ratio of SO_2 to $PM_{2.5}$ from jth emission source. Here, $R_j^{SO_2}$ is an input for the model.

Continuing with the example for SO_2, the relationship between ambient observations and sources of SO_2 can be explained as follows:

$$n \cdot [SO_2]_{ambient} = \sum_{j=1}^{J} [SO_2]_j \tag{7}$$

where $[SO_2]_{ambient}$ is the observed SO_2 concentration, and n is the bound factor. To account for possible transformations (photochemical reactions) of gases during transport (from sources to ambient), we use Eq. (7) as a bound for an acceptable solution (Marmur et al., 2005). According to Marmur's work, the bound factor n is recommended as three.

Thus, the task of CMBGC-Iteration is to resolve Eqs. (5) and (7). Here, the global optimization program is used. The objective of global optimization is to find the best solution of nonlinear decision models with the possibility of multiple locally optimal solutions (Marmur et al., 2005). The MATLAB tool was used to solve the governing source apportionment equations.

Stage (5). Evaluate the convergence of the model.

If $|(s_j^{k+1} - s_j^k)/s_j^{k+1}| > 0.01$, go to stage (2).
If $|(\mathbf{s_j^{k+1} - s_j^k})/\mathbf{s_j^{k+1}}| < \mathbf{0.01}$, convergence, go to stage (6).

Stage (6). Calculate the performance index which is similar to those of EPACMB 8.2 (The USEPA, 2006).

The equations for determining the performance index are described in Eqs. (8)–(10):

$$\sigma_{s_j}^2 = \left(F'\left(V^k\right)^{-1} F_{jj}\right)^{-1} \tag{8}$$

where σ_{si} is the uncertainty of jth source contribution; F is the matrix of source profiles (F' is the transport matrix of F)'; and V^k is the matrix of v. Eq. (9) is described as:

$$\chi^2 = \frac{1}{I - J} \sum_{i=1}^{I} \left[\left(C_i - \sum_{j=1}^{J} \left(f_{ij}\, s_j\right)^2 \Big/ v_i \right] \right. \tag{9}$$

where I is the number of the chemical species used for fitting. A χ^2 value of less than 4 indicates a good result. Eq. (10) is described as:

$$R^2 = 1 - \left[(I-J)\chi^2\right] \Big/ \left[\sum_{i=1}^{n} c_i^2 / v_i\right] \quad (10)$$

where R^2 is in the range of 0–1. A R^2 greater than 0.8 indicates a satisfactory performance.

The CMBGC-Iteration software package was complied using MATLAB which can be freely obtained from the author (nksgl@nankai.edu.cn) or downloaded from authors' research websites (http://env.nankai.edu.cn/air/list/?110_1.html or http://russellgroup.ce.gatech.edu/node/16?destination=node/16).

3. Results and discussion

3.1. Characteristics of air pollutants

3.1.1. Ambient $PM_{2.5}$ and chemical species concentrations

A total of 114 ambient data of $PM_{2.5}$ were obtained by offline sampling from April 2014 to January 2015. The time series of $PM_{2.5}$ concentrations measured in Tianjin is plotted in Fig. 1. The daily $PM_{2.5}$ concentrations ranged from 13 to 275 μg m^{-3}. The annual average concentration of $PM_{2.5}$ was 87 μg m^{-3}, which was different from those in previous studies in Tianjin (Tian et al., 2016b; Wu et al., 2015; Chen et al., 2015). Compared with other regions, the $PM_{2.5}$ concentration levels in this study were lower than those in Beijing (Zíková et al., 2016). In Sun's studies, the average concentration of $PM_{2.5}$ from 1999 to 2011 was 37 μg m^{-3} in Hong Kong (Sun et al., 2015). In New York (USA), the mean $PM_{2.5}$ concentration was only 8 μg m^{-3} (Hopke et al., 2015), which is far lower than that in Tianjin. Knowing this, there are still many actions to be taken to reduce $PM_{2.5}$ emissions. Fall and winter had relatively higher $PM_{2.5}$ concentrations at 118 and 82 μg m^{-3}, respectively, while spring and summer had relatively lower $PM_{2.5}$ concentrations at 66 and 65 μg m^{-3}, respectively. This may be due to the variability in the influence of emission sources and meteorological condition over different seasons.

In this study, 19 major abundant chemical components of $PM_{2.5}$ were analyzed. These chemical components included inorganic elements (Na, Mg, Al, Si, K, Ca, Ti, Cr, Mn, Fe, Ni, Cu, Zn, and Pb), water-soluble ions (SO_4^{2-}, NO_3^-, NH_4^+), and carbonaceous species (organic carbon (OC) and element carbon (EC)). The chemical compositions of $PM_{2.5}$ are exhibited in Table 1. The annual average percentage of the elements was 19% in $PM_{2.5}$. The highest percentage was in autumn at 21%, and the lowest percentage was in winter at 17%. It can be observed that the crustal elements (Al, Si, Ca, Fe, etc.) also exhibited higher fractions: the abundances of Si, Al, Ca, Fe were 5.9%, 2.7%, 3.3%, and 1.9%, respectively. The percentage of water-soluble ions in $PM_{2.5}$ ranged from 25% to 34%, with an annual average percentage of 29%. According to the annual average abundances, the water-soluble ions had significant levels with abundances of 15% (SO_4^{2-}), 7.2% (NO_3^-), and 7.6% (NH_4^+). The carbonaceous species, including OC and EC, accounted for 20% of $PM_{2.5}$. In winter, OC and EC had the highest total percentage of 24%, while

Table 1
Concentrations of chemical species during the sampling campaign.

species	mean (μg m^{-3})	SD[a] (μg m^{-3})	max	min
Na	0.7	0.7	5.1	0.1
Mg	0.6	0.7	4.8	0.0
Al	1.7	1.6	10.8	0.3
Si	4.8	5.4	32.2	0.2
K	1.6	1.3	8.4	0.2
Ca	2.3	2.2	11.1	0.1
Ti	0.1	0.1	0.5	0.0
Cr	0.1	0.1	0.6	0.0
Mn	0.1	0.2	1.7	0.0
Fe	1.4	1.5	0.1	0.1
Ni	0.1	0.1	0.9	0.0
Cu	0.1	0.2	0.9	0.0
Zn	0.5	0.5	2.5	0.0
Pb	0.1	0.1	0.5	0.0
SO_4^{2-}	14.1	13.6	63.4	0.4
NO_3^-	7.6	8.2	34.8	0.1
NH_4^+	7.7	7.3	33.3	0.2
OC	11.8	9.5	60.9	0.7
EC	5.0	5.8	52.6	0.3

[a] SD: standard deviation.

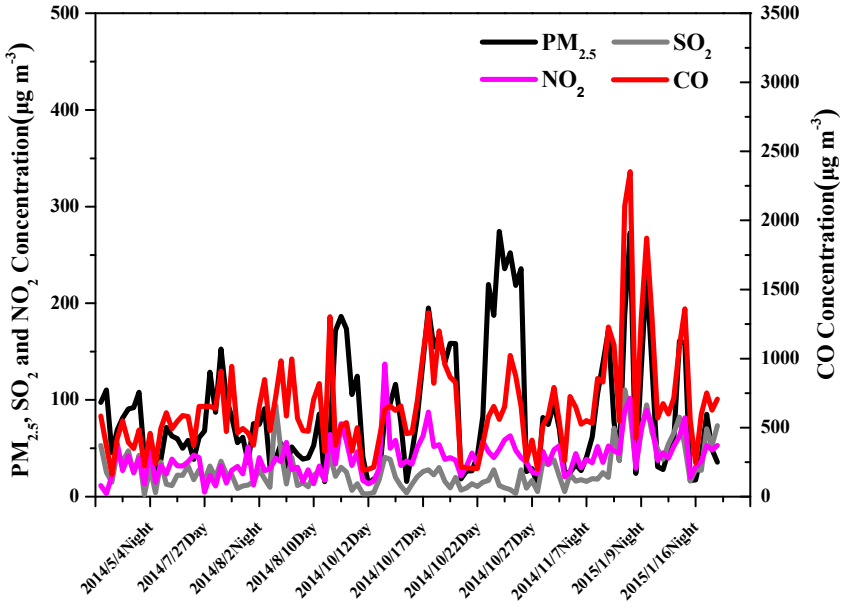

Fig. 1. Time-serial of $PM_{2.5}$ and gaseous pollutants concentrations measured in Tianjin. The black, gray, pink, red lines represent the time series of $PM_{2.5}$, SO_2, NO_2, CO concentrations. (For interpretation of the references to colour in this figure legend, the reader is referred to the web version of this article.)

the lowest percentage was 17% in autumn. The mean OC concentration was 12 μg m^{-3} accounting for 15% of the total $PM_{2.5}$ and 70% of the TC (Total Carbon). EC varied from 0.33 to 19 μg m^{-3} with a mean value of 5.0 μg m^{-3} and contributed to 5.8% of the total $PM_{2.5}$ and 30% of the TC. A similar value was found in previous studies in Tianjin (Gu et al., 2010). Concentrations below the detection limit were replaced by 1/2 of the detection limit values, and their uncertainties were set at 5/6 of the detection limit values (Kim et al., 2003). Missing values were replaced by the geometric mean of the measured values, and their accompanying uncertainties were set at 4 times the mean value (Kim et al., 2003). In this study, 5% of the values were below the detection limit while the missing values accounted for 3%.

In this study, Si, Al, Ca, Fe, SO_4^{2-}, NO_3^-, NH_4^+, OC and EC were the main chemical species in the $PM_{2.5}$, and these components predominantly come from crustal dust, coal combustion, vehicle exhaust, and secondary formation. Si and Ca were more abundant in the spring, due in part to the larger wind speeds increasing crustal dust. SO_4^{2-} fractions were higher in summer due to enhanced photochemical reactions. Additionally, some mass ratios of species, such as NO_3^-/SO_4^{2-} and OC/EC, can be used to interpret the emission and transformation characteristics of atmospheric aerosols. The mass ratio of NO_3^-/SO_4^{2-} is usually utilized to indicate whether mobile sources or stationary sources dominate the contributions to PM pollution (Yao et al., 2002; Qiao et al., 2016). In this study, the average ratio of NO_3^-/SO_4^{2-} was 0.53. In previous studies, the average NO_3^-/SO_4^{2-} in Beijing, Shanghai, Chongqing, and Guangzhou was 0.64, 0.44, 0.21, and 2.1, respectively (Yang et al., 2011). Many studies have pointed out that the OC/EC ratio could indicate the presence of secondary organic carbon (SOC). An OC/EC ratio of 2.2 or 2.0 is usually marks the presence of SOC (Li and Bai, 2009). The average OC/EC ratio of this study was 3.0, which suggested the presence of SOC (Tian et al., 2014). The maximum OC/EC ratio was observed in summer at 3.7, and the minimum was observed in autumn at 2.2, which demonstrated that SOC may play an important role in carbonaceous pollution in Tianjin. The remaining chemical species concentrations were below the detection limit for most samples and were omitted from further analysis.

3.1.2. Characteristics of gaseous pollutants

Some source categories have relatively similar source profiles (e.g., gasoline and diesel vehicles), which may limit the ability of CMB to identify those source impacts accurately. Considering the characteristics of gaseous pollutants, a more reasonable analytical result can be obtained. According to data from National Bureau of Statistics of China in 2014, the total emissions of SO_2, NOx, and particulates in exhaust in Tianjin were 209, 200, 282, 300, and 139,500 tons, respectively. Among them, SO_2 and NOx emissions decreased by 4.0% and 9.0% since 2013. On the contrary, the particulate emissions increased by 59%. The gaseous pollutant concentration data in this study was from online observations. During sampling, the mean concentrations of SO_2, NO_2, and CO were 28, 40, and 651 μg m^{-3}, respectively. The temporal variations of SO_2, NO_2, and CO are shown in Fig. 1. The highest SO_2 concentration occurred in daytime (111 μg m^{-3}). Power plants and industrial combustion may be the dominant contributor to the emissions of SO_2 because the compound can be considered a primary pollutant emitted from coal combustion (Wang and Hao, 2012). Concentrations of NO_2 are usually higher at night than those in the daytime. Therefore, it is reasonable that the NO emitted by anthropogenic sources in daytime was transformed into NO_2 and that NO_2 was accumulated under unfavorable diffusion conditions during night-time (Yang et al., 2015). Chai et al. (2014) studied spatial and temporal variation of gaseous pollutants in 26 cities in China. They found that the six-month average SO_2 concentration was 72 μg m^{-3} in northern cities, which was nearly twice that in the south. CO concentrations in northern and southern China were 240 μg m^{-3} and 100 μg m^{-3}, respectively (Chai et al., 2014).

It was clear that the temporal variations of gaseous pollutant concentrations were consistent with the $PM_{2.5}$ time series to a certain extent, and the time series of these three gaseous pollutants were also consistent (Fig. 1). This situation demonstrated that gaseous pollutant concentrations can reflect the emission sources of $PM_{2.5}$.

3.2. Chemical source profiles

Source profiles of PM are the average relative chemical species of PM from emission sources and are usually expressed as the mass ratio between each species to the total PM (Pernigotti et al., 2016). The chemical composition from different sources is unique, and source profiles reflect the chemical characteristics of the emission sources. According to previous studies and emission inventories, the major source categories used in source apportionment included crustal dust, cement dust, coal combustion, and vehicle exhaust. The profiles of crustal dust, cement dust, coal combustion, and vehicle exhaust were constructed by recent measurement data and measurement methods referred to in our other studies (Bi et al., 2007). The uncertainties of source profiles were derived from the standard deviation of several samples with the same source categories collected in the Tianjin. NO_3^- and SO_4^{2-} were formed from gas- and condensed-phase chemical reactions involving SO_2 and NO_X. The main products were ammonium sulfate and ammonium nitrate. In this study, “pure” ammonium sulfate and ammonium nitrate were used as secondary sulfate and nitrate profiles (Watson et al., 1994, Watson and Chow, 2002; Feng et al., 2007). The SOC profile was 100% OC with a 10% standard deviation, as recommended by the USEPA (The USEPA, 2006). To estimate the formation of secondary pollutants, theoretical profiles were established based on the molecular weight fraction for secondary sulfate, secondary nitrate, and SOC. The details can be seen in our previous studies (Bi et al., 2007). The component bar graphs of each source categories are given in Fig. 2. In crustal dust, Si, Ca, and Al were marker species with percentages of 16%, 8%, and 5%. Ca accounted for 39% in cement dust and was the most important component. Some crustal elements, Ca, Si, and Al (with percentages of 3%, 12%, and 7%) along with SO_4^{2-} (14%), OC (12%), EC (8%), were the dominant species in coal combustion profiles. The marker of secondary sulfate was SO_4^{2-} and accounted for 73%, and NO_3^- had a percentage of 78% and was the main component in secondary nitrate. Secondary sulfate and secondary nitrate make up a greater proportion in $PM_{2.5}$, which were secondary products of SO_2 and NO_X after a series of chemical reactions. The vehicle exhaust profiles were characterized by high percentages of carbonaceous species while OC and EC were the representative species (32% and 30%). OC was a characteristic component in SOC. In the source profiles of this study, the average NO_3^-/SO_4^{2-} ratio was 0.72, and the average OC/EC ratio was 3.7, which were both close to the ratios in ambient $PM_{2.5}$ (0.53 and 3.0).

Some sources would discharge PM as well as gaseous pollutants, and gaseous pollutants can also reflect emission characteristics of pollution sources. Gaseous pollutant emissions information was added in CMBGC and CMBGC-Iteration in the form of gas-to-$PM_{2.5}$ ratios, which helps further identify the source. Gas-to-$PM_{2.5}$ ratios for coal combustion and vehicle exhaust sources were based on the 2014 emission inventory in Tianjin (Table 2). As shown in Table 2, coal combustion was characterized by a significantly higher $SO_2/PM_{2.5}$ ratio than vehicle exhaust. This might be because of sulfur-containing substances in the coal. While the $CO/PM_{2.5}$ ratio in vehicle exhaust was much higher than in coal combustion, this may

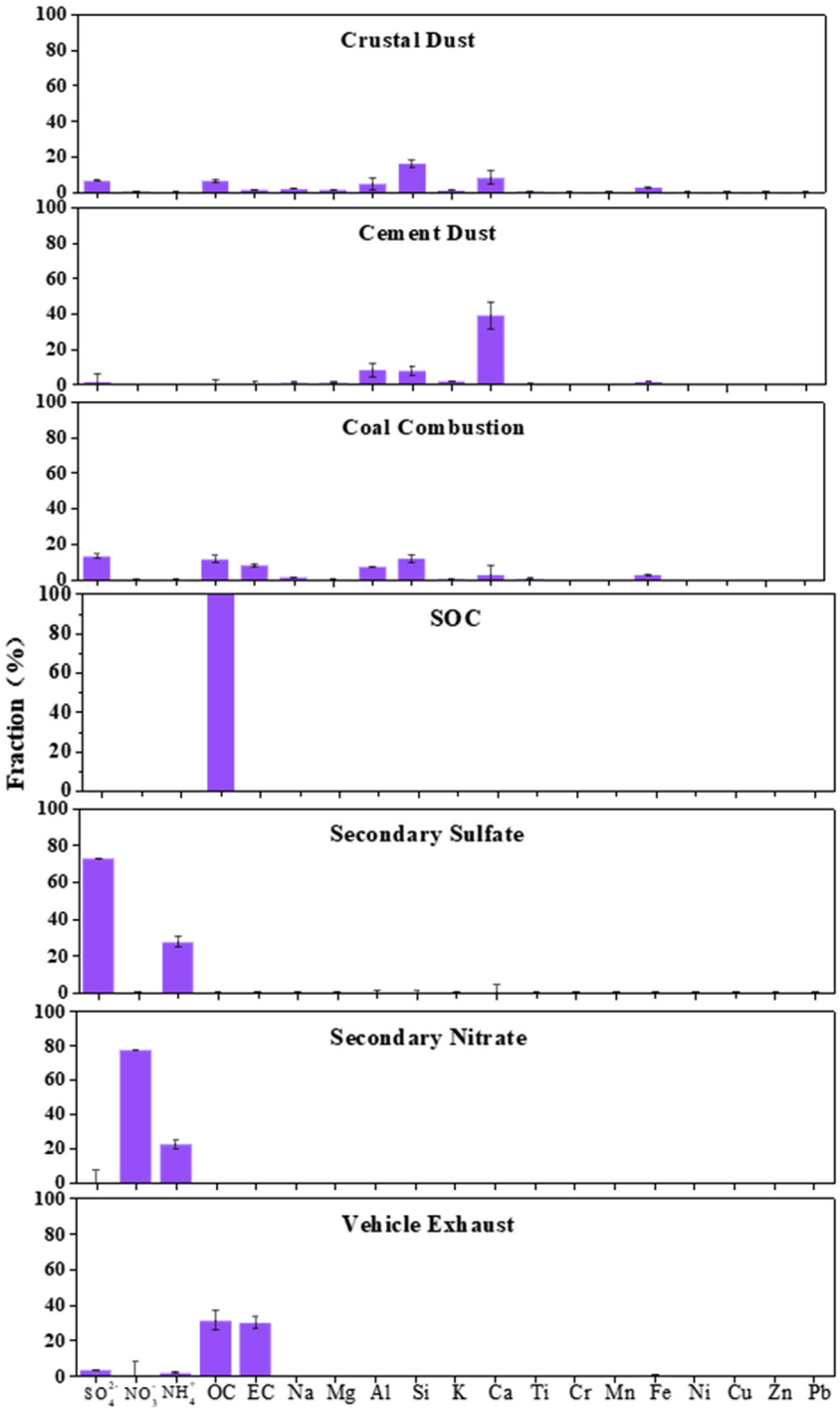

Fig. 2. Source profiles of different kinds of emission sources. The x-axis represents the chemical components, the y-axis represents the percentage, and the purple column is the fraction of the components in the emission sources. (For interpretation of the references to colour in this figure legend, the reader is referred to the web version of this article.)

be caused by incomplete combustion of fuels.

3.3. Source apportionment

In this section, results from the study of an ambient $PM_{2.5}$ dataset are presented, including the improved CMBGC-Iteration model and other receptor model estimates of contributions of potential sources at the ambient site. The receptor models include 1) CMBGC-Iteration, CMBGC, CMB-Iteration and CMB models and 2) multivariate factor analysis models (including PMF, NCAPCA and WALSPMF). The results of different models were compared. The source profiles described in Section 3.2 were used as inputs for four

Table 2
Gas-to-$PM_{2.5}$ ratios used as constraints in the optimization process (mass/mass).

Source	$SO_2/PM_{2.5}$	$CO/PM_{2.5}$	$NOx/PM_{2.5}$
Coal combustion	12.5	3.1	8.3
Vehicle exhaust	2.5	18.3	8.5

chemical mass balance models. Six source categories were identified by the above receptor models: crustal dust, coal combustion, vehicle exhaust, secondary sources (namely secondary sulfate and secondary nitrate), SOC, cement dust, and others.

3.3.1. CMBGC-iteration

3.3.1.1. Source apportionment by CMBGC-Iteration. CMBGC-Iteration is an extension of the traditional CMB model using gas phase species concentration (SO_2, CO and NO_X) as constraints. Compared to CMB-GC, the uncertainties of the ambient dataset and source profiles were involved in the iterative solution of CMBGC-Iteration. The input file for CMBGC-Iteration consisted of concentrations from the ambient dataset, uncertainties of the ambient dataset, source profiles, uncertainties of the source profiles, gas-to-$PM_{2.5}$ ratios, and parameters for solution. The output file contained daily contributions, mean source contributions, a performance index, a Modified Pseudo-Inverse Normalized (MPIN) matrix, modeled species information, and modeled gases information.

Precisely 114 groups of ambient concentration data (including the concentrations of gaseous pollutants) and source profiles were put into the CMBGC-Iteration model, and the mean source contributions of each source category were obtained. The CMBGC-Iteration results of mean source contributions to $PM_{2.5}$ are displayed in Fig. 3. For all potential sources, secondary sources had the largest contribution, accounting for 30% of particle mass concentration. Secondary sources including secondary sulfate and secondary nitrate were formed by chemical reactions of the gaseous precursors (SO_2 and NO_X) and had a major impact on $PM_{2.5}$ levels. In the summer, relatively high temperatures could promote secondary reactions. Crustal dust had the second highest contribution of 25%. More so in spring or fall, crustal dust was the most important source for PM, which may be caused by strong winds that could re-suspend crustal dust (Khan et al., 2010; Tian et al., 2013). The contribution of vehicle exhaust was 16%. The vehicle inventory in Tianjin rose from 840,000 in 2001 to 2.36 million in 2012, an increase of 181%. With the increasing number of vehicles, vehicle exhaust pollution has become an important component of urban air pollution. Coal combustion was also an important source category for $PM_{2.5}$ with an estimated contribution of 13%. Coal consumption grew from 25 million tons in 2001 to 51.62 million tons in 2012, an increase of 107%. SOC contributed 7.6% to $PM_{2.5}$. Cement dust had the lowest contribution, accounting for 0.40%. The low contribution of cement dust might be due to the collinearity with the dust source category.

The performance indices of CMBGC-Iteration model were the same as those of the traditional CMB model, such as reduced chi square (chi^2), R square (R^2), and percent mass (PM) (The USEPA, 2006). In the results of our study, the performance indices (chi^2, R^2, PM) were 0.00, 1.00 and 91.65%, which met the requirement of the CMB model and indicated that the results of iteration were acceptable by CMB model standards.

3.3.1.2. Source apportionment by CMB-GC. The CMB-GC model uses gas phase concentrations to set additional constraints. The source apportionment results by CMBGC are shown in Fig. 3. In the six identified sources, secondary sources gave the highest contribution at 30% with the minimum contribution from cement dust (0.40%). Other source contributions were the following in decreasing order: crustal dust (23%) > vehicle exhaust (15%) > coal combustion (14%) > SOC (8.0%). The same source categories were identified in both CMBGC-Iteration and CMB-GC.

3.3.1.3. Comparing of the results from two models. Fig. 4 shows the source categories identified by CMBGC-Iteration and CMB-GC and the contribution (concentration) of each source. Among the categories, the contributions of secondary sources, SOC, and cement dust were quite similar. For crustal dust and vehicle exhaust, the contributions calculated by CMBGC-Iteration were higher than those by CMB-GC, while the coal combustion contribution obtained by CMBGC-Iteration was lower than that by CMB-GC. The differences in the source apportionment results of the two models were mainly due to the uncertainties of source profiles and observations. According to Eq. (3), the "effective variance" is composed of two parts: the uncertainty of the observations and the uncertainty of the source profiles. It can be seen in Eq. (4) that the weighted concentration of observations and the weighted source profiles are negatively correlated with the effective variance. Therefore, according to Eq. (5), depending on a certain daily concentration of a component, when the uncertainty of this component's concentration in the source profiles increases, the weighted source profile will be reduced. This reduction will cause an increase in the estimated contribution (S_j) of the source that the component contributes highest and a contribution reduction of other sources.

3.3.2. Source apportionment by multiple models

In this section, the ambient receptor data and source profiles were analyzed to study the results of the traditional CMB and CMB-

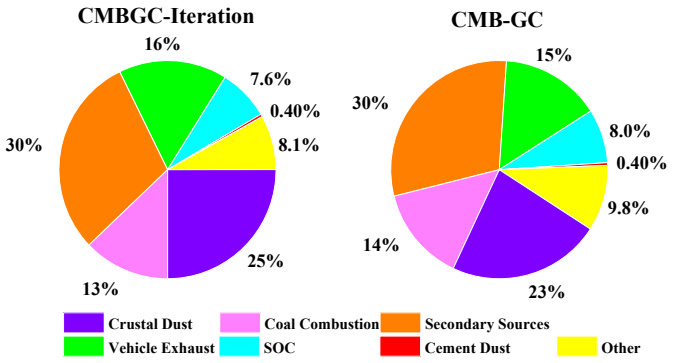

Fig. 3. Source contributions by CMBGC-Iteration and CMB-GC. Different colors represent different source categories. (For interpretation of the references to colour in this figure legend, the reader is referred to the web version of this article.)

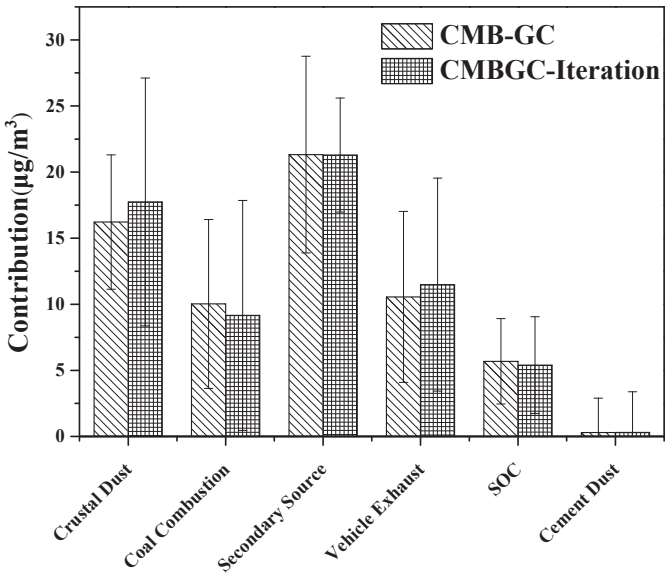

Fig. 4. The comparison of source contributions calculated by CMBGC-Iteration and CMB-GC. The x-axis is the source categories, the y-axis is the source contribution, and the unit is μg m^{-3}.

Iteration models. The source categories, percentage contribution, and performance indices are listed in Table 3. In the traditional CMB model, a pure SOC profile (OC fraction was 100% and other composition fractions were 0%) was used. The source profiles and receptor data would significantly affect the CMB results and cause great uncertainties (Lee and Russell, 2007). The number of source categories identified and the estimated source contributions to $PM_{2.5}$ mass concentrations at the ambient site were almost the same for both CMB and CMB-Iteration. Crustal dust accounted for the largest contribution percentage in both models (27% both in CMB and CMB-Iteration). Cement dust had the smallest contribution percentage at 2.8%. These results are relatively consistent with previous studies (Tian et al., 2016b).

Other models used for source apportionment in this study were PMF, WALSPMF and NCAPCA. Source categories and percentage contributions were resolved by each model with the results listed in Table 3.

A summary of the chemical species introduced into the PMF 5.0 and WALSPMF is displayed in Table 1. Both 114 × 19 receptor concentration matrices and concentration uncertainty matrices were imported into the two models. The factor loadings obtained by PMF are exhibited in Table S1. Four factors were resolved by the PMF model. As shown in Table S1, factor 1 reflected high loading for OC and EC, which are usually markers for vehicle exhaust (Yuan et al., 2006); therefore, this factor might be the vehicle exhaust. In factor 2, SO_4^{2-}, NO_3^-, and NH_4^+ exhibited high weighting, consistent with sources related to secondary sources (Tian et al., 2013). Factor 3 can be associated with Si, Al, Ca, and carbonaceous species, and these species are generally used as the markers for coal combustion (Zhang et al., 2011). Factor 4 had high weighting values for Si, Al, and Ca, which can be treated as markers of crustal dust (Pant and Harrison, 2012); therefore, this factor can be identified as the crustal dust source. As discussed above, the potential sources identified by PMF were vehicle exhaust, secondary sources, coal combustion and crustal dust, and the percentage contributions of each source were 21%, 40%, 25% and 14%, respectively (Table 3). These results were relatively different from those of other models.

Similar to PMF, the WALSPMF model required the concentrations of $PM_{2.5}$ as inputs. Four potential sources were also obtained by WALSPMF (Table 3). The WALSPMF results suggested that secondary source categories were the dominant source, accounting for 29%. The second major source was vehicle exhaust consisting of 27%. The percentage contribution of coal combustion and crustal dust were 26% and 19%, respectively.

The NCAPCA model is a factor analysis model that can estimate the contribution of sources to PM based on the PCA (Principal Component Analysis) method. This model can sometimes produce non-negative contributions. The concentrations of chemical species and $PM_{2.5}$ were introduced into NCAPCA. The NCAPCA model resolved five secondary source categories such as secondary sources, SOC, coal combustion, vehicle exhaust, and crustal dust. The contributions of each source categories are described in Table 3. The secondary source was the highest contributor of $PM_{2.5}$ at 30%. Coal combustion was the second largest contributor at 23%. The other source contributions in descending order are vehicle exhaust (18%) > crustal dust (14%) > SOC (15%).

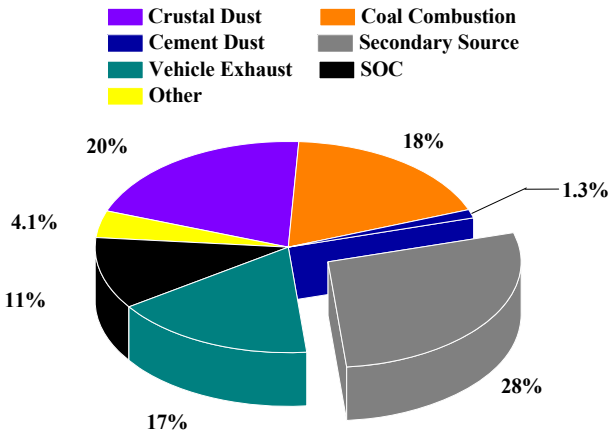

Fig. 5. Ensemble source impacts of multiple receptor models. The seven receptor models were combined to calculate the average ensemble source contributions.

3.4. Results of ensemble source apportionment

CMB, CMB-Iteration, CMB-GC, CMBGC-Iteration, PMF, WALSPMF and NCAPCA results demonstrate that these models can calculate different source contributions for the same ambient data (Fig. 3 and Table 3). The model ensemble used information from seven models whose source impacts could be obtained when an individual model did not provide them. The above seven models were combined to calculate the average ensemble source contributions (Fig. 5). The secondary source (included nitrate and sulfate) was the largest source, accounting for 28%. The second dominant source was crustal dust at 20%. The other source categories contributions in descending order were coal combustion (18%) > vehicle exhaust (17%) > SOC (11%) > cement dust (1.3%). Moreover, the ensemble method also avoided negative and zero value impact estimates for major emissions sources such as vehicles and SOC.

4. Conclusions

Uncertainties of source profiles and receptor datasets are key parameters in source apportionment (SA). To address the uncertainties problem of CMBGC, the CMBGC-Iteration model was developed to include the uncertainties of the ambient dataset and source profiles in the iterative solution. Consequently, the convergence results were obtained, and the source apportionment results were more stable. To apply this model, $PM_{2.5}$ was sampled in Tianjin from April 2014 and January 2015, and chemical species (carbon components, water-soluble ions and elements) in $PM_{2.5}$ were measured by corresponding instruments. Six source

Table 3
Source categories and percentage contributions resolved by different models.

	Contributions (%)							
Source categories	CMB	CMB-Iteration	CMB-GC	CMBGC-Iteration	PMF	WALSPMF	NCAPCA	Ensemble
Crustal Dust	27	27	23	25	14	19	14	20
Coal Combustion	16	16	14	13	25	26	23	18
Secondary Sources	24	24	30	30	40	29	30	28
Vehicle Exhaust	15	15	15	16	21	27	18	17
SOC	6.4	6.4	8.0	7.6	–	–	15	11
Cement Dust	2.8	2.8	0.40	0.40	–	–	–	1.3
Other	9.2	9.2	9.8	8.1	–	–	–	4.1

categories were identified by this model, and their contributions to $PM_{2.5}$ in descending order were secondary sources, crustal dust, vehicle exhaust, coal combustion, SOC, and cement dust.

In addition, six other models, including CMBGC, CMB-Iteration, CMB, PMF, NCAPCA and WALSPMF, were employed to identify the source categories and to estimate the source contributions to $PM_{2.5}$ in Tianjin. Several sources, including crustal dust, cement dust, coal combustion, vehicle exhaust, secondary sulfate, and secondary nitrate were identified. Similar source apportionment results were obtained from the other models, but the number of sources resolved were different for each model. Finally, to obtain more objective SA results, ensemble-average source impacts were calculated based on the seven sets of source apportionment results. Source contributions were similar for the ensemble SA results and CMBGC-Iteration results.

Acknowledgements

This study was supported by the National Natural Science Foundation of China (41775149), National Key Research and Development Program of China (2016YFC0208500, 2016YFC0208505), Special Scientific Research Funds for Environment Protection Commonweal Section (Nos. 201509020, 201409003), the Tianjin Research Program of Application Foundation and Advanced Technology (14JCQNJC0810), Tianjin Natural Science Foundation (17JCYBJC23000, Tianjin Natural Science Foundation (16JCQNJC08700), and the Blue Sky Foundation. This publication was developed under Assistance Agreement No. EPA834799 awarded by the U.S. Environmental Protection Agency to Emory University and Georgia Institute of Technology. It has not been formally reviewed by EPA. The views expressed in this document are solely those of the authors and do not necessarily reflect those of the Agency. EPA does not endorse any products or commercial services mentioned in this publication.

Appendix A. Supplementary data

Supplementary data related to this article can be found at https://doi.org/10.1016/j.envpol.2017.10.007.

References

Arruti, A., Fernandez-Olmo, I., Irabien, A., 2011. Impact of the global economic crisis on metal levels in particulate matter (PM) at an urban area in the Cantabria Region (Northern Spain). Environ. Pollut. 159 (5), 1129–1135.

Bari, M.A., Kindzierski, W.B., 2016. Fine particulate matter ($PM_{2.5}$) in Edmonton, Canada: source apportionment and potential risk for human health. Environ. Pollut. 218, 219–229.

Belis, C.A., Karagulian, F., Larsen, B.R., Hopke, P.K., 2013. Critical review and meta-analysis of ambient particulate matter source apportionment using receptor models in Europe. Atmos. Environ. 69 (3), 94–108.

Belis, C.A., Pernigotti, D., Karagulian, F., Pirovano, G., Larsen, B.R., Gerboles, M., Hopke, P.K., 2015a. A new methodology to assess the performance and uncertainty of source apportionment models in intercomparison exercises. Atmos. Environ. 119, 35–44.

Belis, C.A., Karagulian, F., Amato, F., Almeida, M., Artaxo, P., Beddows, D.C.S., Bernardoni, V., Bove, M.C., Carbone, S., Cesari, D., Contini, D., Cuccia, E., Diapouli, E., Eleftheriadis, K., Favez, O., El Haddad, I., Harrison, R.M., Hellebust, S., Hovorka, J., Jang, E., Jorquera, H., Kammermeier, T., Karl, M., Lucarelli, F., Mooibroek, D., Nava, S., Nojgaard, J.K., Paatero, P., Pandolfi, M., Perrone, M.G., Petit, J.E., Pietrodangelo, A., Pokorna, P., Prati, P., Prevot, A.S.H., Quass, U., Querol, X., Saraga, D., Sciare, J., Sfetsos, A., Valli, G., Vecchi, R., Vestenius, M., Yubero, E., Hopke, P.K., 2015b. A new methodology to assess the performance and uncertainty of source apportionment models II: the results of two European intercomparison exercises. Atmos. Environ. 123, 240–250.

Bi, X.H., Feng, Y.C., Wu, J.H., Wang, Y.Q., Zhu, T., 2007. Source apportionment of PM_{10} in six cities of northern China. Atmos. Environ. 41 (5), 903–912.

Cesari, D., Amato, F., Pandolfi, M., Alastuey, A., Querol, X., Contini, D., 2016a. An inter-comparison of PM10 source apportionment using PCA and PMF receptor models in three European sites. Environ. Sci. Pollut. Res. 23 (15), 15133–15148.

Cesari, D., Donateo, A., Conte, M., Contini, D., 2016b. Inter-comparison of source apportionment of PM_{10} using PMF and CMB in three sites nearby an industrial area in central Italy. Atmos. Res. 182, 282–293.

Chai, F.H., Gao, J., Chen, Z.X., Wang, S.L., Zhang, Y.C., Zhang, J.Q., Zhang, H.F., Yun, Y.R., Ren, C., Shulan, et al., 2014. Spatial and temporal variation of particulate matter and gaseous pollutants in 26 cities in China. J. Environ. Sci. 26 (1), 75–82.

Chen, L.W.A., Watson, J.G., Chow, J.C., Magliano, K.L., 2007. Quantifying $PM_{2.5}$ source contributions for the San Joaquin Valley with multivariate receptor models. Environ. Sci. Technol. 41 (8), 2818–2826.

Chen, P.F., Bi, X.H., Zhang, J.Q., Wu, J.H., Feng, Y.C., 2015. Assessment of heavy metal pollution characteristics and human health risk of exposure to ambient $PM_{2.5}$ in Tianjin, China. Particuology 20, 104–109.

Cheng, H., Sandu, A., 2009. Uncertainty quantification and apportionment in air quality models using the polynomial chaos method. Environ. Modell. Softw. 24, 917–925.

Chow, J.C., Watson, J.G., Lowenthal, D.H., Chen, L.W.A., Zielinska, B., Mazzoleni, L.R., Magliano, K.L., 2007. Evaluation of organic markers for chemical mass balance source apportionment at the Fresno Supersite. Atmos. Chem. Phys. 7, 1741–1754.

de Paula, P.H.M., Mateus, V.L., Araripe, D.R., Duyck, C.B., Saint'Pierre, T.D., Gioda, A., 2015. Biomonitoring of metals for air pollution assessment using a hemi-epiphyte herb (struthanthus flexicaulis). Chemosphere 138, 429–437.

Feng, Y.C., Xue, Y.H., Chen, X.H., Wu, J.H., Zhu, T., Bai, Z.P., Fu, S.T., Gu, C.J., 2007. Source apportionment of ambient total suspended particulates and coarse particulate matter in urban areas of Jiaozuo, China. J. Air Waste Manage 57 (5), 561–575.

Gu, J.X., Bai, Z.P., Liu, A.X., Wu, L.P., Xie, Y.Y., Li, W.F., Dong, H.Y., Zhang, X., 2010. Characterization of atmospheric organic carbon and element carbon of $PM_{2.5}$ and PM_{10} at Tianjin, China. Aerosol Air Qual. Res. 10 (2), 167–176.

Gugamsetty, B., Wei, H., Liu, C.N., Awasthi, A., Hsu, S.C., Tsai, C.J., Roam, A.D., Wu, Y.C., Chen, C.F., 2012. Source characterization and apportionment of PM_{10}, $PM_{2.5}$ and $PM_{0.1}$ by using positive matrix factorization. Aerosol Air Qual. Res. 12, 476–491.

Harrison, R.M., Beddows, D.C., Dall'Osto, M., 2011. PMF analysis of wide-range particle size spectra collected on a major highway. Environ. Sci. Technol. 13, 5522–5528.

Hasheminassab, S., Daher, N., Saffari, A., Wang, D., Ostro, B.D., Sioutas, C., 2014. Spatial and temporal variability of sources of ambient fine particular matter $PM_{2.5}$ in California. Atmos. Chem. Phys. 14 (22), 12085–12097.

Heo, J., Wu, B., Abdeen, Z., Qasrawi, R., Sarnat, J.A., Sharf, G., Shpund, K., Schauer, J.J., 2017. Source apportionments of ambient fine particulate matter in Israeli, Jordanian, and Palestinian cities. Environ. Pollut. 225, 1–11.

Hinwood, A., Callan, A.C., Heyworth, J., Mccafferty, P., Sly, P.D., 2014. Children's personal exposure to PM10 and associated metals in urban, rural and mining activity areas. Chemosphere 108, 125–133.

Hopke, P.K., 2003. Recent developments in receptor modeling. J. Chemom. 17, 255–265.

Hopke, P.K., Kane, C., Utell, M.J., Chalupa, D.C., Kumar, P., Ling, F., Gardner, B., Rich, D.Q., 2015. Triggering of myocardial infarction by increased ambient fine particle concentration: effect modification by source direction. Environ. Res. 142, 374–379.

Kanakidou, M., Seinfeld, J.H., Pandis, S.N., Barnes, I., Dentener, F.J., Facchini, M.C., Van Dingenen, R., Ervens, B., Nenes, A., Nielsen, C.J., 2005. Organic aerosol and global climate modelling: a review. Atmos. Chem. Phys. 5, 1053–1123.

Khan, M.F., Shirasuna, Y., Hirano, K., Masunaga, S., 2010. Characterization of $PM_{2.5}$, $PM_{2.5\text{-}10}$, and $PM_{>10}$, in ambient air, Yokohama, Japan. Atmos. Res. 96, 159–172.

Kim, E., Larson, T.V., Hopke, P.K., Slaughter, C., Sheppard, L.E., Claiborn, C., 2003. Source identification of $PM_{2.5}$ in an arid Northwest US city by positive matrix factorization. Atmos. Res. 66 (4), 291–305.

Kong, S.F., Han, B., Bai, Z.P., Chen, L., Shi, J.W., Xu, Z., 2010a. Receptor modeling of $PM_{2.5}$, PM_{10} and TSP in different seasons and long-range transport analysis at a coastal site of Tianjin, China. Environ. Sci. Technol. 408 (20), 4681–4694.

Kong, S.F., Ding, X., Bai, Z.P., Han, B., Chen, L., Shi, J.W., Li, Z.Y., 2010b. A seasonal study of polycyclic aromatic hydrocarbons in $PM_{2.5}$ and $PM_{2.5\text{-}10}$ in five typical cities of Liaoning province, China. J. Hazard. Mater 1, 70–80.

Kong, S.F., Ji, Y.Q., Liu, L.L., Chen, Li., Zhao, X.Y., Wang, J.J., Bai, Z.P., Sun, Z.R., 2012. Diversities of phthalate esters in suburban agricultural soils and wasteland soil appeared with urbanization in China. Environ. Pollut. 170, 161–168.

Krall, J.R., Anderson, G.B., Dominici, F., Bell, M.L., Peng, R.D., 2013. Short-term exposure to particulate matter constituents and mortality in a national study of US urban communities. Environ. Health. Persp 121 (10), 1148–1153.

Lee, S., Russell, A.G., 2007. Estimating uncertainties and uncertainty contributors of CMB $PM_{2.5}$, source apportionment results. Atmos. Environ. 41 (40), 9616–9624.

Li, W.F., Bai, Z.P., 2009. Characteristics of organic and elemental carbon in atmospheric fine particles in Tianjin, China. Particuology 7 (6), 432–437.

Liberda, E.N., Leonard, J.S., Tsuji, Peltierc, R.E., 2015. Mining in subarctic Canada: airborne $PM_{2.5}$ metal concentrations in two remote first nations communities. Chemosphere 139, 452–460.

Lim, S.S., Vos, T., Flaxman, A.D., Danaei, G., Shibuya, K., Adair-Rohani, H., Amann, M., Anderson, H.R., Andrews, K.G., Aryee, M., 2012. A comparative risk assessment of burden of disease and injury attributable to 67 risk factors and risk factor clusters in 21 regions, 1990-2010: a systematic analysis for the Global Burden of Disease Study 2010. Lancet 380 (9859), 2224–2260.

Louie, P.K.K., Watson, J.G., Chow, J.C., Chen, A., Sin, D.W.M., Lau, A.K.H., 2005. Seasonal characteristics and regional transport of $PM_{2.5}$, in Hong Kong. Atmos. Environ. 39, 1695–1710.

Marmur, A., Unal, A., Mulholland, J.A., Russell, A.G., 2005. Optimization-based

source apportionment of pm2.5 incorporating gas-to-particle ratios. Environ. Sci. Technol. 39 (9), 3245–3255.
Monn, C., 2001. Exposure assessment of air pollutants: a review on spatial heterogeneity and indoor/outdoor/personal exposure to suspended particulate matter, nitrogen dioxide and ozone. Atmos. Environ. 35, 1–32.
Nel, A., 2005. Atmosphere. air pollution-related illness: effects of particles. Science 308, 804–806.
Nelin, T.D., Joseph, A.M., Gorr, M.W., Wold, L.E., 2012. Direct and indirect effects of particulate matter on the cardiovascular system. Toxicol. Lett. 208, 293–299.
Paatero, P., Tapper, U., 1994. Positive matrix factorization: a non-negative factor model with optimal utilization of error estimates of data values. Environmetrics 5, 111–126.
Pant, P.P., Harrison, R.M., 2012. Critical review of receptor modeling for particulate matter: a Case Study of India. Atmos. Environ. 49, 1–12.
Pernigotti, D., Belis, C.A., Spanò, L., 2016. Specieurope:The European data base for PM source profiles. Atmos. Pollut. Res. 7 (2), 307–314.
Qiao, T., Zhao, M.F., Xiu, G.L., Yu, J.Z., 2016. Simultaneous monitoring and compositions analysis of PM_1 and $PM_{2.5}$ in Shanghai: implications for characterization of haze pollution and source apportionment. Sci. Total. Environ. 557, 386–394.
Revuelta, M.A., Mcintosh, G., Pey, J., Pérez, N., Querol, X., Alastuey, A., 2014. Partitioning of magnetic particles in PM_{10}, $PM_{2.5}$ and PM_1 aerosols in the urban atmosphere of Barcelona (Spain). Environ. Pollut. 188, 109–117.
Samara, C., Kouimtzis, T., Tsitouridou, R., Kanias, G., Simeonov, V., 2003. Chemical mass balance source apportionment of PM_{10} in an industrialized urban area of northern Greece. Atmos. Environ. 37 (1), 41–54.
Schauer, J.J., Rogge, W.F., Hildemann, L.M., Hildemann, L.M., Mazurek, M.A., Cass, G.R., 1996. Source apportionment of airborne particulate matter using organic compounds as tracers. Atmos. Environ. 30 (22), 3837–3855.
Seinfeld, J.H., Pandis, S.N., 1998. Atmospheric chemistry and physics: from air pollution to climate change. Environ. Sci. Policy Sustain. Dev. 51 (7), 88–90.
Shi, G.L., Tian, Y.Z., Guo, C.S., Feng, Y.C., Xu, J., Zhang, Y., 2012. Sediment-pore water partition of PAH source contributions to the yellow river using two receptor models. J. Soils Sediments 12, 1154–1163.
Shi, G.L., Liu, G.R., Peng, X., Wang, Y.N., Tian, Y.Z., Wang, W., Feng, Y.C., 2014. A comparison of multiple combined models for source apportionment, including the PCA/MLR-CMB, Unmix-CMB and PMF-CMB models. Aerosol. Air. Qual. Res. 14 (7), 2040. –U341.
Shi, G.L., Peng, X., Liu, J.Y., Tian, Y.Z., Song, D.L., Yu, H.F., Feng, Y.C., Russell, A.G., 2016a. Quantification of long-term primary and secondary source contributions to carbonaceous aerosols. Environ. Pollut. 219, 897–905.
Shi, G.L., Chen, H., Tian, Y.Z., Song, D.L., Zhou, L.D., Chen, F., Yu, H.F., Feng, Y.C., 2016b. Effect of uncertainty on source contributions from the positive matrix factorization model for a source apportionment study. Aerosol Air Qual. Res. 16 (7), 1665–1674.
Singh, N., Murari, V., Kumar, M., Barman, S.C., Banerjee, T., 2017. Fine particulates over South Asia: review and meta-analysis of $PM_{2.5}$ source apportionment through receptor model. Environ. Pollut. 223, 121–136.
Sun, S.Z., Cao, P.H., Chan, K.P., Tsang, H., Wong, C.M., Thach, T.Q., 2015. Temperature as a modifier of the effects of fine particulate matter on acute mortality in Hong Kong. Environ. Pollut. 205, 357–364.
The USEPA, 2006. Technology Transfer Network Support Center for Regulatory Atmospheric Modeling Website. http://wwwepagov/scram001/models/receptor/EPACMB82Manualpdf.
Tian, Y.Z., Wu, J.H., Shi, G.L., Wu, J.Y., Zhang, Y.F., Zhou, L.D., Zhang, P., Feng, Y.C., 2013. Long-term variation of the levels, compositions and sources of size-resolved particulate matter in a megacity in China. Sci. Total Environ. 463, 462–468.
Tian, Y.Z., Wang, J., Peng, X., Shi, G.L., Feng, Y.C., 2014. Estimation of the direct and indirect impacts of fireworks on the physicochemical characteristics of atmospheric PM_{10} and $PM_{2.5}$. Atmos. Chem. Phys. 14 (18), 9469–9479.
Tian, Y.Z., Shi, G.L., Huangfu, Y.Q., Song, D.L., Liu, J.Y., Zhou, L.D., Feng, Y.C., 2016a. Seasonal and regional variations of source contributions for PM_{10} and $PM_{2.5}$ in urban environment. Sci. Total Environ. 557, 697–704.
Tian, Y.Z., Chen, G., Wang, H.T., Huang-Fu, Y.Q., Shi, G.L., Han, B., Feng, Y.C., 2016b. Source regional contributions to $PM_{2.5}$ in a megacity in China using an advanced source regional apportionment method. Chemosphere 147, 256–263.
US-EPA, 1987. In: Protocol for Applying and Validating the CMB Model. Office for Air Quality Planning and Standards.
Van Ryswyk, K., Wheeler, A.J., Wallace, L., Kearney, J., You, H., Kulka, R., Xu, X., 2014. Impact of microenvironments and personal activities on personal $PM_{2.5}$ exposures among asthmatic children. J. Expo. Sci. Environ. Epidemiol. 24, 260–268.
Wang, C.C., Cai, J., Chen, R.J., Shi, J.J., Yang, C.Y., Li, H.C., Li, Z.J., Meng, X., Liu, C., Niu, Y., Xia, Y.J., Zhao, Z.H., Li, W.H., Kan, H.D., 2017. Personal exposure to fine particulate matter, lung function and serum club cell secretory protein (Clara). Environ. Pollut. 225, 450–455.
Wang, S.X., Hao, J.M., 2012. Air quality management in China: issues, challenges, and options. J. Environ. Sci. 24 (1), 2–13.
Watson, J.G., 1984. Overview of receptor model principles. J. Air Waste Manage. Assoc. 34, 619–623.
Watson, J.G., Chow, J.C., Lu, Z.Q., Fujita, E.M., Lowenthal, D.H., Lawson, D.R., 1994. Chemical mass balance source apportionment of PM_{10} during the southern California air quality study. Aerosol Sci. Technol. 21, 1–36.
Watson, J.G., Chow, J.C., Fujita, E.M., 2001. Review of volatile organic compound source apportionment by chemical mass balance. Atmos. Environ. 35 (9), 1567–1584.
Watson, J.G., Zhu, T., Chow, J.C., Engelbrecht, J., Fujita, E.M., Wilson, W.E., 2002. Receptor modeling application framework for particle source apportionment. Chemosphere 49, 1093–1136.
Watson, J.G., Chow, J.C., 2002. Review of $PM_{2.5}$ and PM_{10} apportionment for fossil fuel combustion and other sources by the chemical mass balance receptor model. Energy Fuels 16, 222–260.
Watson, J.G., Chen, L.W.A., Chow, J.C., Doraiswamy, P., Lowenthal, D.H., 2008. Source apportionment: findings from the U.S. supersites program. J. Air Waste Manage. Assoc. 58, 265–288.
Wu, H., Zhang, Y.F., Han, S.Q., Wu, J.H., Bi, X.H., Shi, G.L., Wang, J., Yao, Q., Cai, Z.Y., Liu, J.L., 2015. Vertical characteristics of $PM_{2.5}$ during the heating season in Tianjin, China. Sci. Total Environ. 523, 152–160.
Yang, F., Tan, J., Zhao, Q., Du, Z., He, K., Ma, Y., Duan, F., Chen, G., Zhao, Q., 2011. Characteristics of $PM_{2.5}$ speciation in representative megacities and across China. Atmos. Chem. Phys. 11 (11), 5207–5219.
Yang, J., Nam, I., Yun, H., Kim, J., Oh, H.J., Lee, D., Jeon, S.M., Yoo, S.H., Sohn, J.R., 2015. Characteristics of indoor air quality at urban elementary schools in Seoul, Korea: assessment of effect of surrounding environments. Atmos. Pollut. Res. 6 (6), 1113–1122.
Yao, X.H., Chan, C.K., Fang, M., Cadle, S., Chan, T., Mulawa, P., He, K.B., Ye, B.M., 2002. The water-soluble ionic composition of $PM_{2.5}$ in Shanghai and Beijing, China. Atmos. Environ. 36 (26), 4223–4234.
Yatkin, S., Bayram, A., 2008. Source apportionment of PM_{10} and $PM_{2.5}$ using positive matrix factorization and chemical mass balance in Izmir. Turk. Sci. Total Environ. 390, 109–123.
Yuan, Z.B., Lau, A.K.H., Zhang, H.Y., Yu, J.Z., Louie, P.K.K., Fung, J.C.H., 2006. Identification and spatiotemporal variations of dominant PM_{10} sources over Hong Kong. Atmos. Environ. 40 (10), 1803–1815.
Zhang, Y.F., Xu, H., Tian, Y.Z., Shi, G.L., Zeng, F., Wu, J.H., Zhang, X.Y., Li, X., Zhu, T., Feng, Y.C., 2011. The study on vertical variability of PM_{10} and the possible sources on a 220m tower, in Tianjin, China. Atmos. Environ. 45, 6133–6140.
Zheng, M., Salmon, L.G., Schauer, J.J., Zeng, L., Kiang, C.S., Zhang, Y.H., Cass, G.R., 2005. Seasonal trends in $PM_{2.5}$ source contributions in Beijing, China. Atmos. Environ. 39, 3967–3976.
Zheng, M., Cass, G.R., Ke, L., Wang, F., Schauer, J.J., Edgerton, E.S., Russell, A.G., 2007. Source apportionment of daily fine particulate matter at Jefferson Street, Atlanta, GA, during summer and winter. J. Air Waste Manage 57 (2), 228–242.
Zhou, J., Ito, K., Lall, R., Lippmann, M., Thurston, G., 2011. Time-series analysis of mortality effects of fine participate matter components in Detroit and Seattle. Environ. Health. Persp 119 (4), 461–466.
Zíková, N., Wang, Y.G., Yang, F.M., Li, X.H., Tian, M., Hopke, P.K., 2016. On the source contribution to Beijing $PM_{2.5}$, concentrations. Atmos. Environ. 134, 84–95.